FEBS Letters 587 (2013) 912–916

journal homepage: www.FEBSLetters.org

Effect of cargo size and shape on the transport efficiency of the bacterial Tat translocase

Neal Whitaker, Umesh Bageshwar, Siegfried M. Musser *

Department of Molecular and Cellular Medicine, College of Medicine, The Texas A&M Health Science Center, 1114 TAMU, College Station, TX 77843, USA

ARTICLE INFO

Article history:
Received 19 December 2012
Revised 5 February 2013
Accepted 7 February 2013
Available online 16 February 2013

Edited by Stuart Ferguson

Keywords:
Secretion
Bacteria
Inverted membrane vesicle
Twin arginine translocation

ABSTRACT

The Tat machinery translocates fully-folded and oligomeric substrates. The passage of large, bulky cargos across an ion-tight membrane suggests the need to match pore and cargo size, and therefore that Tat transport efficiency may depend on both cargo size and shape. A series of cargos of different sizes and shapes were generated using the natural Tat substrate pre-SufI as a base. Four (of 17) cargos transported with significant (>20% of wild-type) efficiencies. These results indicate that cargo size and shape significantly influence Tat transportability.

1. Introduction

The twin arginine translocation (Tat) machinery transports fully-folded and assembled cargos from the *Escherichia coli* cytoplasm to the periplasm [1]. In the predominant model of Tat-dependent transport, cargos first interact with a receptor complex comprised of TatB and TatC, and then are conveyed across the bilayer though a channel composed primarily of TatA [2,3]. The signal peptide is removed after transport by a periplasmic peptidase resulting in the mature form of the protein [4].

The Tat machinery can potentially be used to produce protein products [5,6]. For increased ease and rapidity of purification, the bacterial Sec system has long been used to transport proteins of interest into the periplasm or outside of the cell [7]. The Sec system, however, cannot transport proteins that are oligomeric or fast-folding, or that require cytoplasmic reagents for cofactor assembly and insertion. The Tat translocase offers an attractive alternative pathway that, in principle, could accommodate these problematic substrates. Additionally, the Tat translocase possesses a poorly understood quality control mechanism that appears to be able to prevent incorrectly folded cargos from transporting, which would presumably allow for isolation of only correctly folded proteins [8,9]. In order to make efficient use of the Tat system in this way, it is important to understand the limitations of the machinery, especially its capability to translocate unnatural substrates.

The Tat system's ability to transport hetero-oligomeric proteins with only a single signal peptide has been termed the "hitch-hiker" mechanism. For example, the small (HybO) and large (HybC) subunits of *E. coli* hydrogenase 2 are transported together, with HybO responsible for the co-transport of HybC [10]. The catalytic dimer of dimethyl sulfoxide reductase (DmsAB) also has only a single signal peptide, which is found on DmsA [11]. Despite the presence of these naturally occurring hitch-hiker complexes, efforts to transport "unnatural" non-covalent hetero-dimers have been unsuccessful. Two studies that address this directly utilized biotinylated natural cargo bound to avidin tetramers. In both instances, the proteins (OE17 and SufI) failed to transport under in vitro conditions, despite binding to the Tat translocon [12,13]. These bound, non-transportable cargos were not, however, dead-end intermediates (i.e., they were not "stuck" in the translocon) because they could be exchanged for different cargos that were subsequently transported.

The size limitations of the Tat machinery have been probed with natural Tat substrates or signal peptides fused to a separate protein domain. When the natural chloroplast Tat substrate OE17 was fused to a Protein A moiety separated by varying lengths of unstructured linkers [14], the fused cargos failed to fully transport. The fusions with the longest linkers formed membrane spanning intermediates that were not associated with the translocon. Green fluorescent protein (GFP) was translocated into inverted membrane vesicles (IMVs) containing the *E. coli* Tat system when it was fused to the signal peptide of pre-TorA [15], but it did not transport or even bind to the translocon when it was fused to the signal peptide of pre-SufI [15].

* Corresponding author. Fax: +1 979 847 9481.
E-mail address: smusser@tamu.edu (S.M. Musser).

0014-5793/$36.00
http://dx.doi.org/10.1016/j.febslet.2013.02.015

The above studies suggest that Tat transport efficiency depends on cargo size, shape, and even the mature domain itself. Consequently, we probed Tat translocation efficiency with various modified forms of the natural cargo pre-SufI of different sizes and shapes, ensuring that the core signal peptide and mature domain recognition motifs remained present. We used a GFP fusion and non-covalent pre-SufI-avidin hetero-dimers formed from biotinylated versions of single cysteine mutants [16]. The naturally occurring, high affinity, dimeric avidin homolog, rhizavidin, was compared with tetrameric avidin [17]. Our results indicate that transport efficiency is dependent on both molecular weight and shape.

2. Methods

2.1. Bacterial strains, plasmids, and growth conditions

IMVs were prepared from *E. coli* strain MC4100ΔTatABCDE overexpressing TatA, TatB and TatC from plasmid pTatABC by induction with 0.6% arabinose, as previously described [15,16].

Plasmid pPre-SufI-GFP was generated by PCR amplification of the GFP gene from plasmid spTorA-GFP [15] using primers 5′-AAAACTCGAGGATCGGCGCAAGCGGCGCGTAAAGGA-3′ (forward) and 5′-AAAAGCTAGCTTTGTATAGTTCATCCATGACCATGCCATGTC-3′ (reverse), which introduced two flanking restriction sites (*Nhe*I and *Xho*I). The GFP gene was inserted into pSufI-MCC [13] at *Nhe*I/*Xho*I between the coding sequences for pre-SufI and the 6xHis tag. A frame shift error was corrected by *Xho*I digestion and Klenow fragment fill-in (Fig. S1). Because the pre-SufI-GFP fusion protein is too large to be readily distinguished on an SDS–PAGE gel from the mature SufI-GFP protein, the coding sequence for pre-SufI-GFP was inserted into pTYB11 (New England Biolabs) with *Sap*I/*Nhe*I generating pIntein-pre-SufI-GFP (Fig. S2), which allowed purification of only the full length precursor, as described previously [16].

The pre-SufI single cysteine mutants necessary for the pre-SufI^{biotin} experiments were produced as described previously [16]. The rhizavidin expression plasmid was a gift from Barbara Niederhauser [17].

2.2. Protein purification, labeling and detection

Pre-SufI cysteine mutants and pre-SufI-GFP were expressed and purified, as described [16]. Cysteines were biotinylated with *N*-(3-maleimidylpropionyl)biocytin (Invitrogen) [13]. Rhizavidin was purified as described [17], and labeled with Alexa532-succinimide with a 20-fold molar excess of dye for 1 h at room temperature in 100 mM sodium bicarbonate (pH 8.25). The reaction was quenched with 100 mM Tris–HCl (pH 8.0), final concentration. Excess dye was removed by spin filtration with addition of fresh bicarbonate buffer after each spin (8 consecutive 5 min spins at 10000 rcf) using Pall Nanosep Omega spin-filters (3000 MW cut-off). Untransported rhizavidin could not be removed by proteinase K digestion, due to the protein's resistance to proteolytic digestion [17], so it was removed by centrifugation with translocation buffer containing 2 M urea and 1 M KCl to separate the pre-SufI/rhizavidin complex from the IMVs [13]. The term "avidin" refers to the glycosylation free variant NeutrAvidin (Invitrogen).

Most proteins were detected by Western blotting using avidin-HRP and chemilumescence [13]. Rhizavidin^{Alexa532} was detected by in-gel fluorescence imaging (model FX PhosphorImager, Bio-Rad Laboratories). In Fig. 2, pre-SufI and pre-SufI-GFP were detected by anti-SufI immunoblotting.

2.3. Transport reactions

Protein translocation assays were performed essentially as described [15]. Unless otherwise noted, initial precursor concentrations were 90 nM. Errors are reported as S.E.M. IMV concentration was standardized using the absorbance at 280 nm in 2% SDS [15]. For all translocation reaction reported here, A_{280} = 5.

3. Results

3.1. Pre-SufI cargos

The natural Tat substrate, pre-SufI, was selected as a template for a series of cargos based on its relatively high transport efficiency [13,15]. For initial experiments, GFP was fused to the pre-SufI C-terminus, generating a cargo with a molecular weight of 86 kDa. C-terminal fusions with authentic Tat cargos have been described earlier [12,14,18]. Our goal, however, was to examine Tat transport efficiency for a range of cargos that differed not only in size, but in shape. To this end, a series of 8 single cysteine mutants were utilized (Fig. 1). When the biotinylated pre-SufI mutants were mixed with saturating levels of avidin, the pre-SufI^{biotin}/avidin complexes all had a MW of ~113 kDa, but with 8 distinct morphologies.

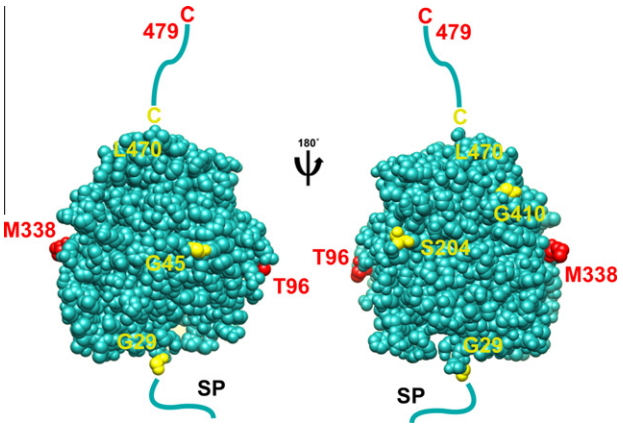

Fig. 1. Location of single cysteine mutations on the surface of pre-SufI. Sites where residues were mutated to cysteine are indicated in red or yellow (PDB accession number: 2UXT). Biotinylated mutants that had transport efficiencies >20% in the presence of rhizavidin (Fig. 3C) are identified in red. All other cysteine locations are yellow.

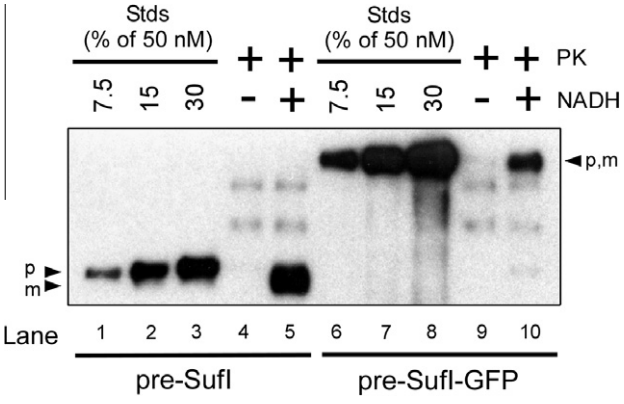

Fig. 2. Pre-SufI-GFP transports with limited efficiency. In vitro transport assays with 50 nM pre-SufI (lanes 1–5) and pre-SufI-GFP (lanes 6–10). Precursor (p) and matured (m) protein bands are identified. Pre-SufI-GFP transported ~17% as efficiently as pre-SufI (compare lane 10 to lane 5), based on the concentration standards (lanes 1–3 and 6–8). Lanes 4 and 9 are minus PMF controls. Proteinase K was added to lanes 4, 5, 9, and 10. Bands were visualized by anti-SufI immunoblotting.

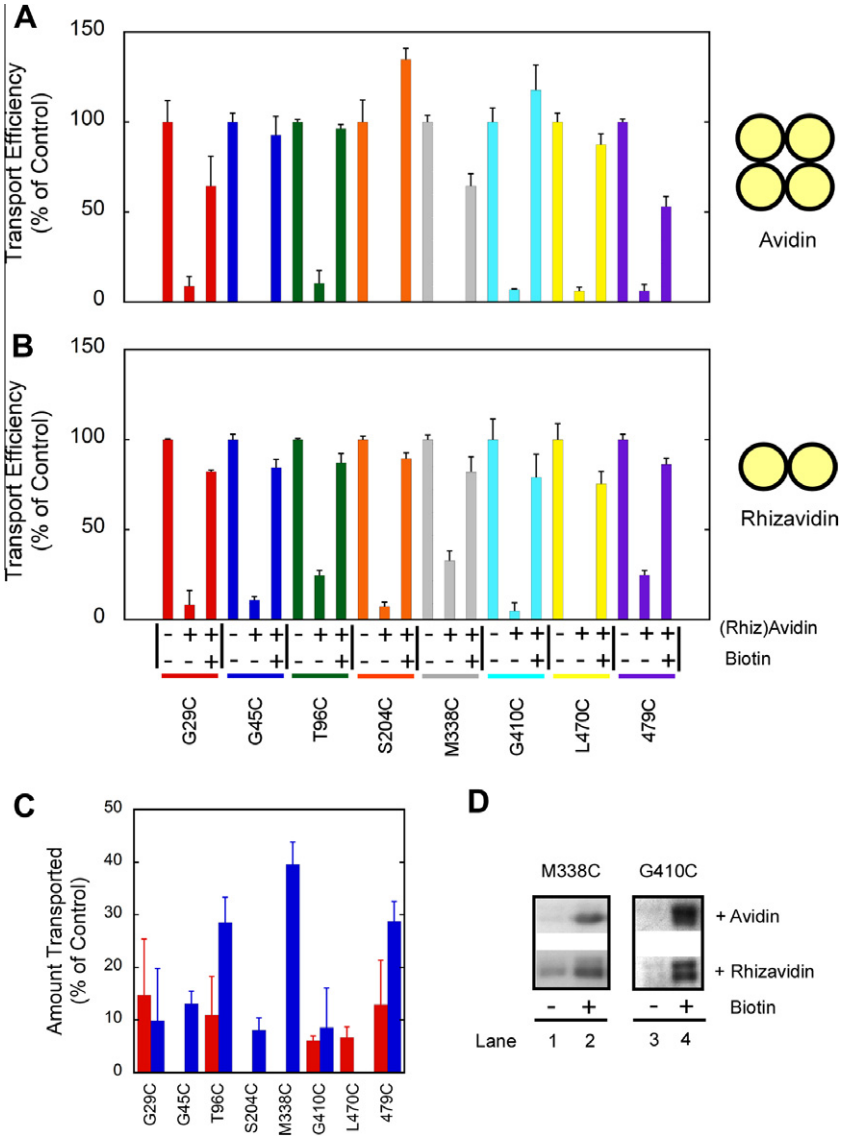

Fig. 3. Pre-SufI^{biotin} transports in the presence of rhizavidin with limited and shape-dependent efficiency. (A&B) Pre-SufI^{biotin} transport efficiency in the presence of (A) avidin tetramers and (B) rhizavidin dimers. When present, biotin (36 μM) was in large excess over (rhiz)avidin (3.6 μM), and (rhiz)avidin was in large excess over the precursor protein (90 nM, 3.1 pmol). Thus, the binding interactions were saturated. The graphs represent an average of three independent experiments, normalized to transport in the absence of (rhiz)avidin and biotin (control). (C) Transport efficiency of the pre-SufI^{biotin} mutants in the presence of avidin (*red*) and rhizavidin (*blue*), calculated by comparing + and − biotin conditions. (D) An example of the transport reactions in (A) and (B) for a pre-SufI^{biotin} mutant that transported in the presence of rhizavidin, but not avidin (M338C), and a mutant that did not transport under either condition (G410C). All reactions were energized with NADH. Proteins were detected by Western blotting using avidin-HRP.

Rhizavidin, found in the nitrogen-fixing bacterium *Rhizobium etli,* is a naturally occurring, dimeric homolog of avidin. It does not have the 1–2 and 1–3 interfaces that tetrameric avidin has, yet it still maintains a high affinity for biotin [17,19]. Complexes of the biotinylated pre-SufI mutants and rhizavidin have a MW of ~83 kDa.

3.2. Transport efficiencies of modified pre-SufI proteins

Transport efficiencies for all pre-SufI constructs were measured using the in vitro transport assay described previously, which relies on the appearance of a protease protected mature protein [15]. In short, cargo protein was mixed with IMVs containing over-expressed TatABC. Membranes were energized by addition of NADH, which promotes translocation of the cargo into the lumen of the vesicles. After 30 min, reactions were treated with Proteinase K, which digests any untranslocated cargo. The resultant mixtures were resolved via SDS–PAGE and visualized by Western blotting.

Pre-SufI-GFP was inefficiently transported (17% of wild-type SufI; Fig. 2). Since GFP is not transported when fused to the SufI signal peptide, but it is transported when fused to the TorA signal peptide [15], these data indicate that the mature domain of pre-SufI plays an important role in the ability of the translocon to transport the GFP domain.

Transport efficiencies were also determined for the biotinylated pre-SufI single cysteine mutants in the presence of avidin or rhizavidin (Fig. 3). All pre-SufI^{biotin} proteins transported inefficiently, or not at all, when bound to the avidin tetramer (Fig. 3A), consistent with our previous report on a C-terminally biotinylated pre-SufI protein [13]. Rhizavidin was also highly effective in blocking transport, though, in some cases, significantly less effective than avidin

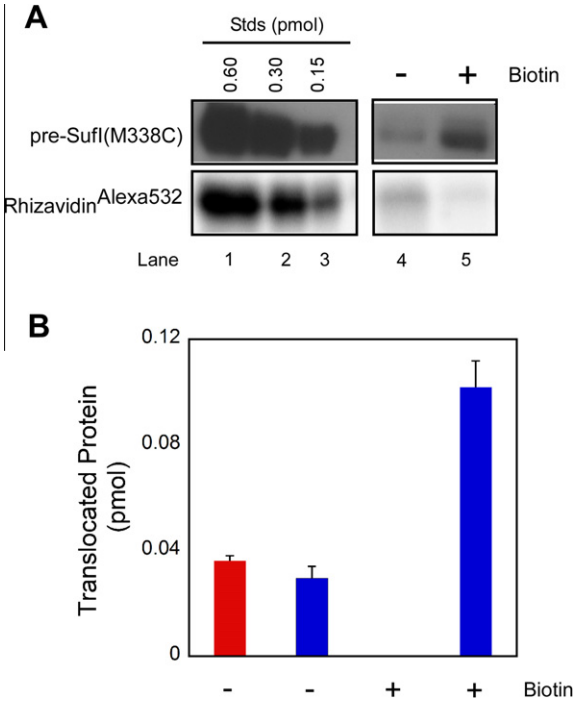

Fig. 4. Rhizavidin is translocated into the lumen of IMVs. (A) Transport of pre-SufI(M338C)^{biotin} in the presence of rhizavidin^{Alexa532}. Lanes 4 and 5 show the amount of IMV-associated SufI(M338C)^{biotin} (top) or rhizavidin^{Alexa532} (bottom). Instead of protease treatment, IMVs were washed with KCl/urea (see Methods). Biotin (36 μM) was absent/present as indicated. Pre-SufI(M338C)^{biotin} was detected by Western blotting using avidin-HRP (top), and rhizavidin^{Alexa532} was detected by in-gel fluorescence imaging (bottom). Lanes 1–3 are concentration standards. (B) Bar graph of averaged data of the type shown in (A), showing the total amount of transported rhizavidin (*red*) and pre-SufI (*blue*) ($N = 3$). The transported rhizavidin in the presence of excess biotin was below the quantifiable range and taken to be zero.

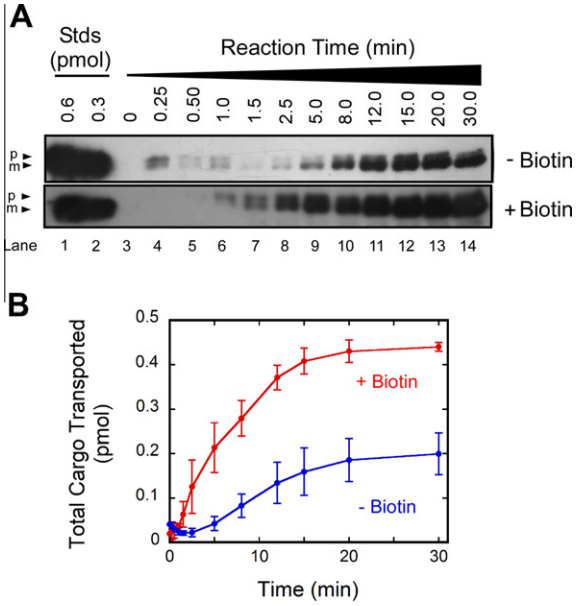

Fig. 5. Transport kinetics of pre-SufI(M338C)^{biotin} in the presence and absence of bound rhizavidin. (A) Time courses of pre-SufI(M338C)^{biotin} translocation in the presence of 3.6 μM rhizavidin and either the presence (bottom gel) or absence (top gel) of 36 μM biotin. Reactions were performed at 37 °C by removing aliquots at the time points indicated and adding them to chilled tubes containing nigericin and valinomycin (5 μM final of each) to quench the reactions. Bands were visualized by Western blotting using avidin-HRP. The exposure times are different, so intensities are not directly comparable. (B) Quantification of kinetic data like that in (A). The amount of transported protein for the 30 min timepoint was determined by comparison to concentration standards, and was then used to determine the amount of transported protein at the remaining timepoints. Only the mature length protein (m) was quantified ($N = 3$).

(Fig. 3B). To confirm that the effects of (rhiz)avidin were due to specific interactions with biotin and to correct for any possible effects of (rhiz)avidin on transport, control experiments were performed in which free biotin was added before (rhiz)avidin (Fig. 3A and B). Transport efficiencies were then calculated relative to this free biotin control for both avidin and rhizavidin (Fig. 3C). Using this definition, the transport efficiencies for all pre-SufI^{biotin}/avidin complexes were ⩽15%. However, transport efficiencies of 28%, 39%, and 28% were observed in the presence of rhizavidin for the T96C, M338C, and T479C mutants, respectively (Fig. 3C).

Based on the high affinity of the biotin-avidin interaction ($K_D \approx 10^{-15}$ M, which predicts τ_{off} on the order of days) [20], the pre-SufI^{biotin}/avidin complexes were expected to remain intact during in vitro Tat dependent transport, which takes place within a few minutes [16]. To test whether the pre-SufI^{biotin}/avidin complex was transported intact, we assayed for the presence of fluorescent rhizavidin (rhizavidin^{Alexa532}) in the IMV lumen for the most efficiently transported pre-SufI mutant. More rhizavidin was recovered with IMVs in the absence than in the presence of free biotin (Fig. 4). Thus, more rhizavidin was recovered with the IMVs under conditions where it is able to bind to the precursor protein. It is unlikely that the *N*-(3-maleimidylpropionyl)biocytin linker (~2 nm in length) was able to span the lipid bilayer, allowing the pre-SufI protein to be transported while leaving the rhizavidin outside. Thus, we conclude that rhizavidin was transported into the IMV lumen while bound to pre-SufI(M338C)^{biotin}. We had some difficulty with complete removal of untransported cargo protein without protease digestion. This may account, at least in part, for the higher amount of transported cargo than the transported rhizavidin. However, it is also possible that some unbound pre-SufI was transported despite a 10-fold molar excess of rhizavidin.

Transport efficiencies were calculated by determining the amount of transported protein at a single time point (30 min). To test whether lower pre-SufI^{biotin} transport efficiencies in the presence of rhizavidin can be explained by slower transport rates, the time dependence of pre-SufI(M338C)^{biotin} transport in the presence and absence of bound rhizavidin were compared (Fig. 5A). In both the presence and absence of bound rhizavidin, the amount of transported SufI(M338C)^{biotin} saturated at ~20 min (Fig. 5B), indicating that the single time point data (30 min) accurately reports overall transport efficiency.

4. Discussion

Previous studies of Tat cargo translocation efficiencies have probed the role of the overall molecular weight and the total length of a linker between two folded domains [14,21]. The current study has methodically examined, for the first time, the Tat machinery's ability to transport cargos of different sizes and shapes, while attempting to minimize changes to the overall charge of the protein, the surface charge, the signal peptide, and the ability of the translocon to bind to the signal peptide. Our major findings are that the size of linked protein and the location of the linkage between two folded domains spaced by a short (~2 nm) linker significantly affects cargo transport efficiency. These data therefore indicate that the overall size and shape of a cargo vis-à-vis the signal peptide are important for the Tat machinery's ability to accommodate a cargo for transport.

In all cases, the presence of a bound avidin tetramer substantially inhibited pre-SufI^{biotin} transport (⩽15% of wildtype; Fig. 3A). In most cases, the transport inhibition by rhizavidin was

$\leqslant$ the inhibition by avidin. The L470C mutant appears to be an exception, but the quantification of very low transport efficiencies, which are determined from fluorescent gels, are somewhat error-prone. In addition to the size differences of avidin and rhizavidin, their pI's (6.3 and 4.0, respectively) and/or different surface charge distributions may also contribute to interactions with the Tat transport system. Proteins larger than the pre-SufI^{biotin}/avidin complexes appear to be transported under natural conditions [22]. In our in vitro experiments, the duration, and possibly the magnitude, of the membrane potential are not as high or as long as they are expected to be under in vivo conditions. So, higher energetic input could be required for the transport of larger proteins, as concluded earlier [21].

The various pre-SufI^{biotin}/rhizavidin complexes had highly variable transport efficiencies (from 0 to 40%; Fig. 3C). Residue modification does not explain these results. Alexa532 labeling at the pre-SufI single cysteine sites had little effect on transport (>80% of wildtype), although a slightly greater effect was observed near the signal peptide (G29C and G45C, 66–75% of wildtype) [16]. Attachment of biotin at these cysteines had little effect on transport ($\geqslant$85% of wildtype, not shown). Thus, the poor transport of the pre-SufI^{biotin}/rhizavidin complexes is most likely due to the rhizavidin domain bound to the biotin moiety, and the range of transport efficiencies is most likely due to the different three-dimensional shapes vis-à-vis the signal peptide when the complexes are presented to the Tat system for transport. The three mutations that yielded the highest transport efficiencies in the presence of rhizavidin, T96C, M338C, and 479C, are widely dispersed over the preSufI surface. T96 and M338 are on opposite sides, and residue 479 is on the side opposite of the signal peptide (Fig. 1). Since the S204C and G45C mutations are similarly distant from the signal peptide as T96C and M338C, i.e., near the 'equator' in Fig. 1, we suggest that the cargo is likely not allowed to freely rotate when bound to the Tat translocon. No transport of the L470C mutant was detected, indicating that the flexible linker between L470 and 479C is crucial for the transport machinery to accommodate a rhizavidin domain attached to the 479 position.

The transport kinetics of pre-SufI(M338C)^{biotin}/rhizavidin were examined (Fig. 5) to determine whether the lower observed transport efficiencies determined from single timepoint data (Fig. 3) could be explained by a slower transport rate. The amount of transported pre-SufI(M338C)^{biotin}/rhizavidin complex clearly plateaued at a lower overall transport efficiency as compared to the rhizavidin-free precursor protein, indicating that longer reaction times would not result in more translocated cargo. Further work will be required to identify the exact effect of cargo shape on transport efficiency.

The Tat machinery's ability to translocate folded and oligomeric proteins will likely continue to attract attention for the production and purification of proteins that cannot be secreted by the more commonly used Sec system. This study implies that not every tightly folded protein can be secreted by the Tat machinery when coupled to a readily recognizable transportable carrier cargo. Thus, we still have much to learn about the recognition, size, and shape requirements of Tat cargos.

5. Disclosure summary

The authors have no conflicts of interest to disclose.

Acknowledgments

We thank T.L. Yahr for pTatABC, T. Palmer for MC4100ΔTatABCDE, and B. Niederhauser for the rhizavidin expression plasmid. This research was supported by the NIH (GM065534).

Appendix A. Supplementary data

Supplementary data associated with this article can be found, in the online version, at http://dx.doi.org/10.1016/j.febslet.2013.02.015.

References

[1] Clark, S.A. and Theg, S.M. (1997) A folded protein can be transported across the chloroplast envelope and thylakoid membranes. Mol. Biol. Cell 8, 923–934.
[2] De Leeuw, E., Porcelli, I., Sargent, F., Palmer, T. and Berks, B.C. (2001) Membrane interactions and self-association of the TatA and TatB components of the twin-arginine translocation pathway. FEBS Lett. 506, 143–148.
[3] Gohlke, U., Pullan, L., McDevitt, C.A., Porcelli, I., de Leeuw, E., Palmer, T., Saibil, H.R. and Berks, B.C. (2005) The TatA component of the twin-arginine protein transport system forms channel complexes of variable diameter. Proc. Natl. Acad. Sci. USA 102, 10482–10486.
[4] Luke, I., Handford, J.I., Palmer, T. and Sargent, F. (2009) Proteolytic processing of *Escherichia coli* twin-arginine signal peptides by LepB. Arch. Microbiol. 191, 919–925.
[5] Bruser, T. (2007) The twin-arginine translocation system and its capability for protein secretion in biotechnological protein production. Appl. Microbiol. Biotechnol. 76, 35–45.
[6] Yoon, S.H., Kim, S.K. and Kim, J.F. (2010) Secretory production of recombinant proteins in *Escherichia coli*. Recent Pat. Biotechnol. 4, 23–29.
[7] Mergulhao, F.J., Summers, D.K. and Monteiro, G.A. (2005) Recombinant protein secretion in *Escherichia coli*. Biotechnol. Adv. 23, 177–202.
[8] Rocco, M.A., Waraho-Zhmayev, D. and Delisa, M.P. (2012) Twin-arginine translocase mutations that suppress folding quality control and permit export of misfolded substrate proteins. Proc. Natl. Acad. Sci. USA 109, 13392–13397.
[9] Sargent, F. (2007) Constructing the wonders of the bacterial world: biosynthesis of complex enzymes. Microbiology 153, 633–651.
[10] Rodrigue, A., Chanal, A., Beck, K., Muller, M. and Wu, L.F. (1999) Co-translocation of a periplasmic enzyme complex by a hitchhiker mechanism through the bacterial Tat pathway. J. Biol. Chem. 274, 13223–13228.
[11] Sambasivarao, D., Turner, R.J., Simala-Grant, J.L., Shaw, G., Hu, J. and Weiner, J.H. (2000) Multiple roles for the twin arginine leader sequence of dimethyl sulfoxide reductase of *Escherichia coli*. J. Biol. Chem. 275, 22526–22531.
[12] Musser, S.M. and Theg, S.M. (2000) Characterization of the early steps of OE17 precursor transport by the thylakoid DeltapH/Tat machinery. Eur. J. Biochem. 267, 2588–2598.
[13] Bageshwar, U.K., Whitaker, N., Liang, F.C. and Musser, S.M. (2009) Interconvertibility of lipid- and translocon-bound forms of the bacterial Tat precursor pre-SufI. Mol. Microbiol. 74, 209–226.
[14] Cline, K. and McCaffery, M. (2007) Evidence for a dynamic and transient pathway through the TAT protein transport machinery. EMBO J. 26, 3039–3049.
[15] Bageshwar, U.K. and Musser, S.M. (2007) Two electrical potential-dependent steps are required for transport by the *Escherichia coli* Tat machinery. J. Cell Biol. 179, 87–99.
[16] Whitaker, N., Bageshwar, U.K. and Musser, S.M. (2012) Kinetics of precursor interactions with the bacterial Tat translocase detected by real-time FRET. J. Biol. Chem. 287, 11252–11260.
[17] Helppolainen, S.H., Nurminen, K.P., Maatta, J.A., Halling, K.K., Slotte, J.P., Huhtala, T., Liimatainen, T., Yla-Herttuala, S., Airenne, K.J., Narvanen, A., Janis, J., Vainiotalo, P., Valjakka, J., Kulomaa, M.S. and Nordlund, H.R. (2007) Rhizavidin from *Rhizobium etli*: the first natural dimer in the avidin protein family. Biochem. J. 405, 397–405.
[18] Lindenstrauss, U. and Bruser, T. (2009) Tat transport of linker-containing proteins in *Escherichia coli*. FEMS Microbiol. Lett. 295, 135–140.
[19] Meir, A., Helppolainen, S.H., Podoly, E., Nordlund, H.R., Hytonen, V.P., Maatta, J.A., Wilchek, M., Bayer, E.A., Kulomaa, M.S. and Livnah, O. (2009) Crystal structure of rhizavidin: insights into the enigmatic high-affinity interaction of an innate biotin-binding protein dimer. J. Mol. Biol. 386, 379–390.
[20] Strunz, T., Oroszlan, K., Schumakovitch, I., Guntherodt, H. and Hegner, M. (2000) Model energy landscapes and the force-induced dissociation of ligand-receptor bonds. Biophys. J. 79, 1206–1212.
[21] Alder, N.N. and Theg, S.M. (2003) Energetics of protein transport across biological membranes. a study of the thylakoid DeltapH-dependent/cpTat pathway. Cell 112, 231–242.
[22] Palmer, T., Sargent, F. and Berks, B.C. (2005) Export of complex cofactor-containing proteins by the bacterial Tat pathway. Trends Microbiol. 13, 175–180.

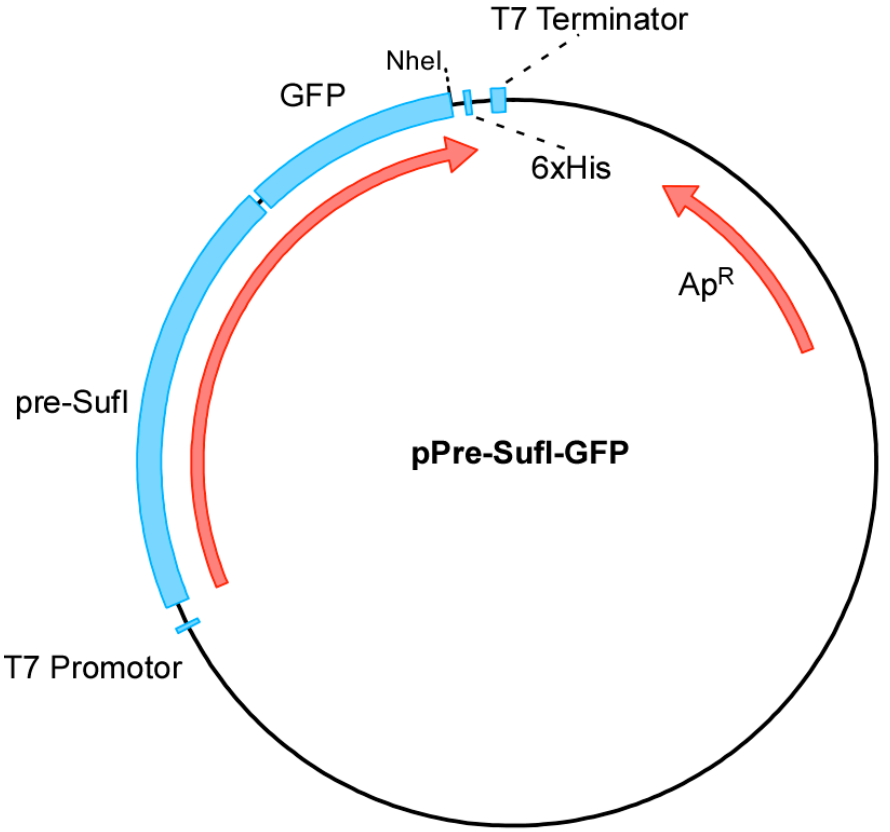

pre-SufI

5'-TACCGCTCGATCGAGGATCGGCGCAAGCGGCG

GFP **NheI**

CGTAAAGGAG.....ACAAAGCTAGCCAC-3'

Figure S1. Plasmid map of pPre-SufI-GFP. The GFP gene was inserted after the C-terminus of pre-SufI with a 21 bp linker, but before the 6xHis tag sequence.

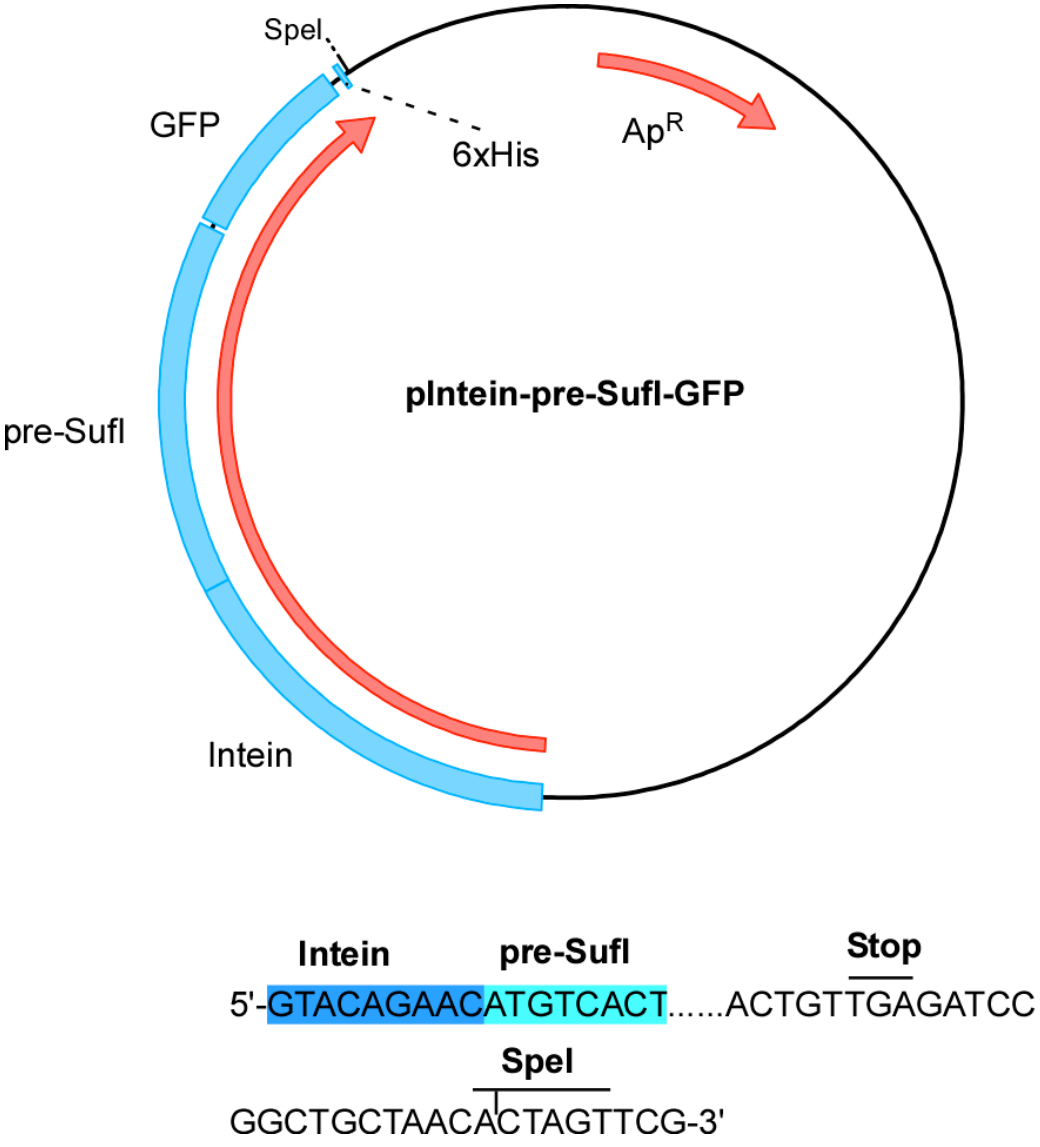

Figure S2. Plasmid map of pIntein-pre-SufI-GFP. The plasmid pIntein-pre-SufI-GFP was generated by inserting the coding sequence for pre-SufI-GFP from plasmid pPre-SufI-GFP into the vector pTYB11 (New England Biolabs) at restriction enzyme sites *Sap*I and *Spe*I. Since *Sap*I does not cleave at the restriction enzyme recognition site, the recognition sequence was lost after insertion of the pre-SufI sequence.